A closer look at IRSL SAR fading data and their implication for luminescence dating – Final Response

Annette Kadereit[1)], Sebastian Kreutzer[2), 3)], Christoph Schmidt[4), 5)]

[1)] Heidelberger Lumineszenzlabor, Geographisches Institut, Universität Heidelberg, Im Neuenheimer Feld 348, 69120 Heidelberg, Germany

[2)] Geography & Earth Sciences, Aberystwyth University, Aberystwyth, SY23 3DB, United Kingdom

[3)] IRAMAT-CRP2A, UMR 5060, CNRS-Université Bordeaux Montaigne, Pessac, France

[4)] Lehrstuhl Geomorphologie, Universität Bayreuth, Universitätsstr. 30, 95447 Bayreuth, Germany

[5)] University of Lausanne, Institute of Earth Surface Dynamics, Quartier UNIL-Mouline, Bâtiment Géopolis, CH-1015 Lausanne

We thank the anonymous reviewers for their thoughtful comments. Basically, the reviewers argue that our observations may be owed to (1) the x-axis scaling in the figures and (2) the use of polymineral fine grains instead of (K-)feldspar coarse grains. Therefore, we re-analyzed our data, created graphs as commonly used for g-value[1] estimations and accomplished our SAR[2] IRSL fading measurements by SAR post-$IR_{1st}IR_{2nd}$ fading measurements, both on polymineral fine-grains and feldspar coarse grains. In short, the phenomenon of an initial (semi-)plateau exists and applies also to $pIR_{1st}IR_{2nd}$ as well as feldspar coarse grains. As pointed out by the reviewers, g-values from $pIR_{1st}IR_{2nd}$ measurements above zero may be measurement artifacts (cf. also Thiel et al. 2011). Our $pIR_{1st}IR_{2nd}$ measurements give hints on how such artifacts could possibly be generated. However, during the data reanalysis we also learned that the steering software of the luminescence reader behaved in an unexpected way and that therefore we cannot stick to the original interpretation that the shape of the fading curve may be attributed to varying heat assistance. For this reason, we have to withdraw our manuscript. Nevertheless, we would like to share our experience, so that nobody else will repeat the same mistake (section 2). Further, we share some of our reanalyzed IRSL data (section 3) and newly acquired $pIR_{1st}IR_{2nd}$ data (section 4). We will start with a consideration on the graphical presentation (section 1).

1 Plots and x-axis scaling

As our observations had made us suspicious of the data curves we did not calculate any g-values from them in the manuscript, as this did not seem appropriate. We decided to leave the data as unprocessed as possible. This is why we used gross signals instead of net signals and merely ensured that both signals follow the same trend. From our perspective now, this procedure was crude but ok. But we also used a rough approach for the scaling of the x-axis. Instead of plotting decades ($\log_{10}[t/tc]$)[3] we plotted the „pauses“ as typed in the sequence editor on a logarithmic scale. This allowed a better visual inspection of the data points of the short pauses which are too cramped and undecipherable otherwise (**Fig. 1a** vs **1b**). In order to compare the initial prompt readouts with the final prompt readouts we plotted the first close to zero, as explained in the manuscript, and the latter after a breach in the x-axis. As we did not perform any calculations, modelling or other mathematically-based analyses on the data and as we did not

[1] denoting the percentage fading loss of a luminescence signal per decade (e.g., Aitken 1985)

[2] Single aliquot regenerative (Murray & Wintle 2000)

[3] tc denoting the prompt readout and t denoting any delayed readout

want to overload the manuscript with more graphs (zooms, insets) we had decided for this „shortcut“.

Our measurements were originally carried out with an old Risø TL/OSL DA12 system with a software emulator. In this system, the BIN-file does not provide information on the „time since irradiation“. Thus we used the pause-times from the sequence, later also for data obtained with the DA20 reader. It is obvious, that this crude approach neglects the offset of the „prompt“ delay time, which includes half the irradiation time, time for cooling, moving of the turntable, heating, liftup and so forth. In the case of the SAR IRSL measurements of our study this delay time adds up to ca. 280 s. But as shown in **Fig. 1a**, which considers this offset (and the normalisation to the prompt readout (tc)), this does not significantly transform the shape of the fading curve. Please note that the graphs with a logarithmic x-axis in the final response do not show the zero-values, which is a clear disadvantage in view of a desirable quick optical inspection of the complete SAR measurement from the initial to the final prompt readouts. Nevertheless, the logarithmic scale allows for better optical inspection (e.g., identification of inflexion points) of the early part of the fading curve than a linear scale. The thin grey line connecting the data points serves as a guide for the eye.

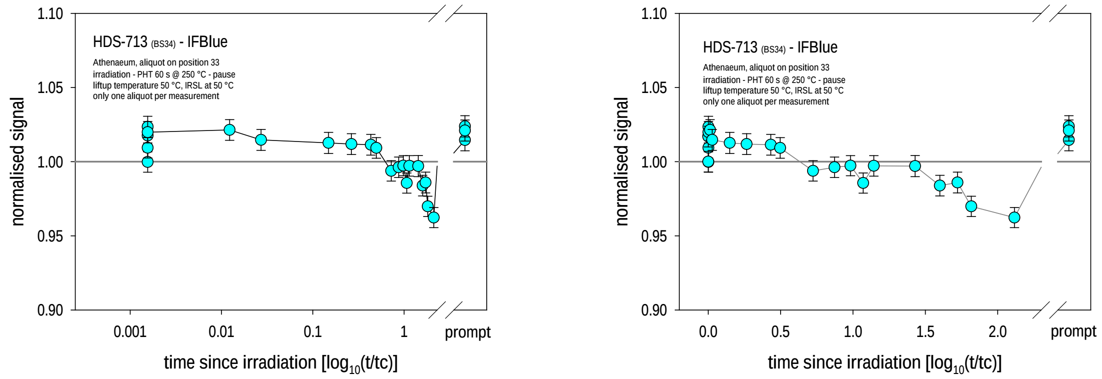

(a) **(b)**

Fig. 1 Results for sample HDS-713 on reader DA20 (Athenaeum) with preheat 60 s at 250 °C, IRSL readout at 50 °C, liftup temperature 50 °C. Laboratory dose 10.3 Gy (100 s beta irradiation time) and normalisation dose 5.2 Gy (50 s beta irradiation time). T_{fad}-15 (each aliquot measured separately in three individual sequences), aliquot 3. Time since irradiation ($\log_{10}$ [t/tc]) plotted on **(a)** a logarithmic scale and **(b)** a linear scale, as conventionally used for g-value estimation.

2 An unexpected finding - pauses are not processed as expected

Our original idea was to present data and a first visual interpretation, but not to calculate any g-values from them. However, after having received the reviews from GChron we re-analysed the data we had compiled in the manuscript with the function „analyse_FadingMeasurement()“ of the R package „Luminescence“ (developer version 0.9.8.9000-17, Kreutzer & Burow 2020). For illustrative purposes the data from R were further processed with SigmaPlot (v11.0). This time, however, we worked off the measurements in a reversed order, starting with those on reader DA20 which did provide the „times since irradiation“. Surprisingly, the results showed in the beginning of each measurement a larger number of (up to ca. 7) data points for $\log_{10}$(t/tc) around 0 (indicating prompt readout) than would correspond to the three initial dose points associated with a „pause“ (sequence editor) of 0 s. This means that data points which in the original manuscript version had been plotted „prompt, prompt, prompt, 10 s, 20 s (and perhaps 30 s, 40 s) all represent „prompt“ readouts. What could be the reason?

It appears that this was due to an unexpected behaviour of the reader software. We assumed that a “pause of x s” in a sequence essentially adds a “pause of time x s” to the measurement. This, however, was not the case as shown by the two following screenshots (**Fig. 2**). **Fig. 2a** shows the sequence screenshot for which all run cells are identical, except for row three where the pause increases from 0 s to 60 s. However, as **Fig. 2b** shows, the corresponding time since irradiation (right column) was always around 280 s and increased only with run 10, by 8 s, while the actually requested pause in run 10 was 50 s. Why is this so?

Several reasons are possible including that the data in the column “time since irradiation” (**Fig. 2b**) is not correct. Although this might be possible we do not regard this as likely.

Run 4	Run 5	Run 6	Run 7	Run 8	Run 9	Run 10	Run 11
Beta 100s	Beta 100s	Beta 100s	Beta 100s	Beta 100s	Beta 100s	Beta 100s	Beta 100s
Pre Heat 250°C;10°C/s;60s	Pre Heat 250°C;10°C/s;60s	Pre Heat 250°C;10°C/s;60s	Pre Heat 250°C;10°C/s;60s	Pre Heat 250°C;10°C/s;60s	Pre Heat 250°C;10°C/s;60s	Pre Heat 250°C;10°C/s;60s	Pre Heat 250°C;10°C
Pause 0s	Pause 0s	Pause 10s	Pause 20s	Pause 30s	Pause 40s	Pause 50s	Pause 60s
OSL 50°C IR LEDs;240.00s;5°	OSL 50°C IR LEDs;240.00s;5°	OSL 50°C IR LEDs;240.00s;5°	OSL 50°C IR LEDs;240.00s;5°	OSL 50°C IR LEDs;240.00s;5°	OSL 50°C IR LEDs;240.00s;5°	OSL 50°C IR LEDs;240.00s;5°	OSL 50°C IR LEDs;2

(a)

POSITION	LTYPE	RUN	SET	TIMESINCEIRR
All	All	All	All	All
21	IRSL	1	5	278
21	IRSL	2	5	279
21	IRSL	3	5	279
21	IRSL	4	5	280
21	IRSL	5	5	279
21	IRSL	6	5	280
21	IRSL	7	5	280
21	IRSL	8	5	280
21	IRSL	9	5	279
21	IRSL	10	5	288
21	IRSL	11	5	298
21	IRSL	12	5	395

(b)

Fig. 2 Screenshots for comparing **(a)** the input in the sequence editor with **(b)** the processed measurement sequence. Here cut-out Run 4 to Run 11, Set 1 to Set 3.

Assuming that the data in the BIN-file are correct (**Fig. 2b**) we consider the following assumption as most likely: After preheating (or any other measurement step involving increased temperature) the reader needs some time to cool down to the set threshold of the liftup temperature. As however „pauses“ (and here we can only speculate, as we do not know the source code) are likely not a step for which it is checked whether or not the liftup temperature has already been reached before a pause starts, pauses may become part of the idle time of the cool-down process. This way short pauses may become completely „used up“ by the cool-down process (cool-down time > pause), and only longer pauses (pause > cool-down time) will effectively elongate the delay time. If this consideration is correct, the very early plateaus as presented in the manuscript are merely artefacts. These very early plateaus do not exist (hereafter „fake plateaus“). On reader DA20 the first (up to ca. 7) data points need to be transferred to 0 ($\log_{10}$ [t/tc]) on the x-axis (or 0 s „delay IRSL-readout“ in the manuscript version). On reader DA12 up to ca. 20 data points are affected representing the very short pauses, which were in steps of 1 s.

Unfortunately, we were not aware of this unexpected software design, which made us investigate shorter and even shorter delay times, down to 1 s on reader DA12, and assume that thermal assistance of the IRSL readout after very short and short delay times causes the emergence of an initial plateau in the fading curves. As this interpretation can not be kept up we can not proceed with a publication of our data in GChron but have to withdraw the manuscript.

Whatever the reasons for the unexpected processing of the input data in the sequence editor are and regardless of the fact that aliquots are not “lifted up” on the heating plate during “pauses”, we would appreciate a software which treats all pauses in the same way.

Despite this drawback, our experiments have produced valuable data. Although the very tips of the initial plateaus, the “fake plateaus”, disappear to condense into an unexpected large number of initial prompt readouts, the fading curves still exhibit an initial plateau (**Fig. 3f**).

3 Calculating g-values from our SAR IRSL measurements

For the g-value calculations with the R package „Luminescence“ we used an early integral of 1–20 s and a late-light subtraction of 201–240 s. The graphs show colour-coded lines to indicate selected sections of the curves and the resulting g-values if those sections are used for g-value determination. Stars serve the same purpose. In those cases, we did not use entire sections of the curves, but only the points highlighted by means of the star symbols.

Our maximum delay times are too short for reliable g-value calculation. The numeric values, however, support the optical inspection of the shape of the fading curves. This way, the g-values serve as a proxy, similar to the numerical expression indicating the slope of a regression line.

The results are summarised as follows:

- Including three final prompt readouts serves to monitor the overal stability of the SAR measurement. In our case, including or excluding the final three prompt readouts for g-value estimation does not change the numerical results significantly. The g-value calculations appear quite robust in this respect.
- Most measurements seem to show an initial plateau, a less steeper gradient or a kind of flat-step stair („semi-plateau“) up to ca. 0.5 decades, which is sometimes shorter and sometimes longer. In this part of the fading curve g-values may be smaller than for the subsequent part and/or for the complete data set, as indicated by few arbitrarily given examples in **Fig. 3** and **Fig. 4**.
- Generally, the numeric data (g-values) support the visual impression of an initial (semi-) plateau. This finding conforms to Visocekas (1985, 1993) and Huntley & Lamothe (2001) who exclude fading shortly after irradiation and to Auclair et al. (2003) who showed that effects of thermal electron transfer may overprint anomalous fading if preheating is performed immediately before the IRSL readout.
- As indicated by the examples supplemented by red star signatures (three initial prompt readouts, one data point towards the end of the initial plateau, two data points representing the two longest delay times): If only very few data points are used and one of these sits near the end of the initial plateau this may slightly increase the g-value as compared to the complete data set (grey and light blue lines and numbers). This corroborates to Huntley & Lamothe (2001) who argue that the log-time equation does not apply to very short times.

- This finding also confirms our concern – expressed in the manuscript and being motivation for compiling our data for peer review – that measuring only few data points may have an influence on the g-value calculation. In that case the relative position of the prompt readout weighs particularly, especially if for better precision it is repeated several times.
- The fading test with the most intense preheat procedure of 60 s at 280 °C (**Fig. 4d–f**) still shows the stretching and finally updoming of the early part of the fading curve from aliquot 1 to aliquot 3. As many of the early values of the normalised signal are above one (overshooting for aliquot 3 up to ca. 1 – 1.5 decades) this does not allow reasonable g-value calculation for these fading curves. It seems that the electron redistribution lasts up to ca. 1.6 decades (here 11075 s or ca. 3 hours, respectively, in a test with 100 s laboratory irradiation and tc = 265 s) if stronger preheating procedures are applied. Or do we observe here another and/or additional effect?
- Although preheating after the delay time (prior to IRSL-readout; Rhodius et al. 2015) instead of preheating before the delay time (immediately after laboratory irradiation; Auclair et al. 2003) reduces the overall g-value, the fading curve still exhibits an initial (semi-)plateau (T_{fad}-16, **Fig. 2 j-l**). This seems to suggest that in addition to electron redistribution due to preheating (Auclair et al. 2003), which affects each data point in equal measure, other charge transfer processes could be responsible for the formation of an initial plateau and appear to be the dominating effect. Huntley & Lamothe (2001) argue that short recombination times would correspond to short distances between trap and recombination centers in the crystal lattice, which however become more and more unlikely with decreasing distance. Non-fading would be the result.

If the observation of an initial plateau is accepted, this would lead to the question of how to correctly handle the „prompt“ readout. The position of the prompt readout may vary even for fading tests with equal laboratory irradiation times as, among others, the delay time for the earliest readout depends on the time of preheating and the time for reaching the liftup temperature. Therefore „prompt“ is relative, but never immediate, and the data of the „prompt“ readout is part of the (very early part of the) initial plateau, as observed in our measurements. In fact, it is the earliest measurable data point of the here detected (semi-)plateau, but not its origin.

Therefore the question arises: If the geologically relevant fading meachnism does not act on short delay times, is it correct to include the prompt readouts in the g-value calculation? In practice, this procedure serves to define the g-value slope most precisely close to the point of origin, but does it also define it accurately? Or do we get a higher precision at the expense of a less correct result?

If the „prompt“ readout occured immediately after the laboratory irradiation or the preheating, one could possibly argue that electron redistribution has not yet fully started and therefore may possibly be neglected. But comparing tc with the length of time of the laboratory irradiation (half the time according to Auclair et al. 2003) plus the time for preheating shows that this assumption is not valid. Also, our fading curves show that the „prompt“ dose points are part of the initial (semi-)plateau – although there are cases in which electron redistribution may increase (normalized IRSL signals > 1) for short but longer-than-prompt delay times.

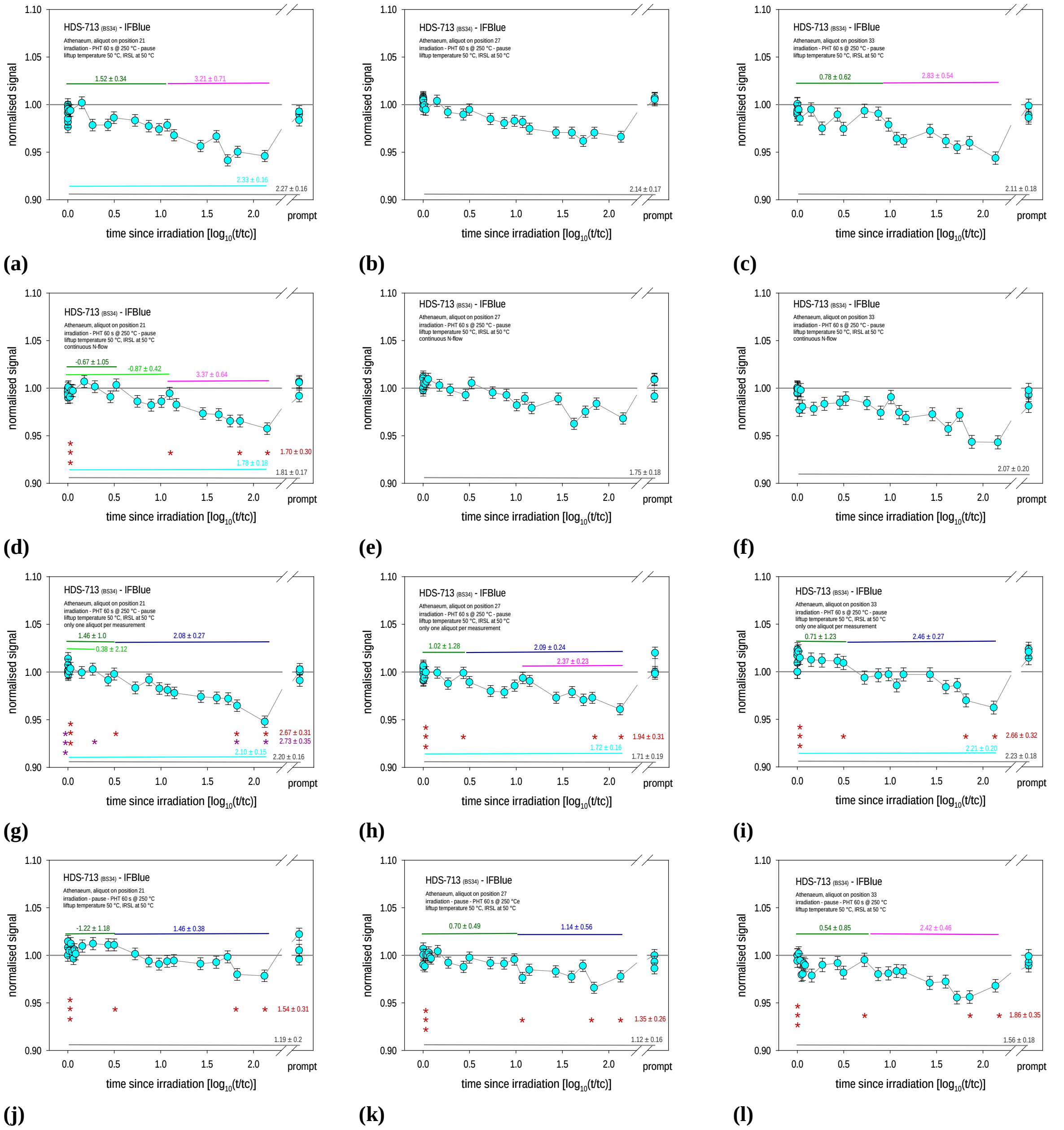

Fig 3 Results for HDS-713 on DA20 (Athenaeum) with preheat 60 s at 250 °C, IRSL readout at 50 °C, liftup temperature 50 °C. Laboratory dose 10.3 Gy (100 s beta irradiation time) and normalisation dose 5.2 Gy (50 s beta irradiation time). Graphs arbitrarily supplemented with g-values for parts of the fading curves and for selected data points.

- **(a – c)** only 120 s nitrogen flow at the beginning (T_{fad}-13)
- **(d – f)** continuous nitrogen flow (T_{fad}-14)
- **(g – i)** each aliquot measured separately in three individual sequences (T_{fad}-15)
- **(j – l)** pause before preheat (Rhodius et al. 2015) (T_{fad}-16)

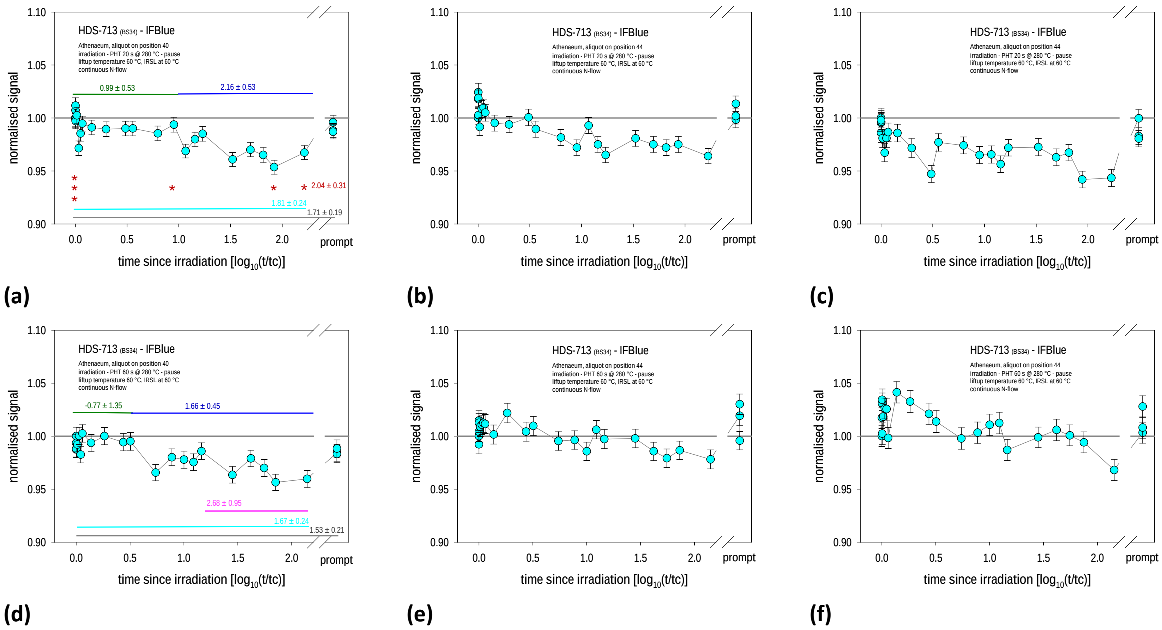

Fig 4 Results for HDS-713 on DA20 (Athenaeum) with IRSL readout at 60 °C and liftup temperature 60 °C. Laboratory dose 10.3 Gy (100 s beta irradiation time) and normalisation dose 5.2 Gy (50 s beta irradiation time). Graphs arbitrarily supplemented with g-values for parts of the fading curves and for selected data points.

- **(a – c)** Preheat 20 s at 280 °C (T_{fad}-17) *versus* **(d – f)** preheat 60 s at 280 °C (T_{fad}-18).

4 $pIR_{1st}IR_{2nd}$-tests on polymineral fine grains and feldspar coarse grains

For our study we had chosen polymineral fine grains assuming that potential inter-aliquot heterogeneity which may occur with coarse grains can be excluded for fine grains with several 10^5 grains per aliquot. Further, not only fine grains but coarse-grain separates, too, contain different kinds of feldspar as (1) in practice sample preparation is not specific enough and (2) individual feldspar grains exhibit phase-exsolution lamellae. Nevertheless, we considered it worth investigating the reviewer's idea that our observations could be a specification of our fine grains, which are irrelevant for coarse grains.

4.1 Methodical details

We performed a fading test on three aliquots of feldspar coarse grains (150–200 µm), using: Norfloat Potash Feldspar, G-40 Feldspar and F-20 Feldspar with likely potassium contents (KO_2) of 12.0 wt.-%, 10.4 wt.-% and 4.1 wt.-%, respectively (cf. **Table i** in the appendix). The material was only resieved but not further processed (e.g., no etching). The test was performed on another Risø luminescence reader model TL/OSL DA20 (No. 245; same specifications as the reader used for the IRSL tests on the polymineral fine grains) utilizing small aliquots with few 10^1 grains each fixed with silicon spray (hole mask ø 1 mm) on aluminium cups (ø ca. 10 mm).

This time, however, for the fading test a post-IR IRSL approach (Thomsen et al. 2008) was applied using a preheat of 60 s at 280 °C, IRSL at 60 °C for 240 s and post-IR IRSL at 225 °C for 240 s ($pIR_{60}IR_{225}$). The test was performed after one-time 2 minutes N-purge at the beginning.

For comparison with polymineral fine grains we also performed $pIR_{60}IR_{225}$-tests on another sample of the loess-borne sediments from SW-Germany (HDS-511; drilling core HBIII, 750 – 757 cm; Kadereit et al. 2011). These tests were performed with different modes of N use. Here we give an example of a measurement with repeated N-purge (2 minutes N-purge after each SAR cycle).

To compensate for the loss of intensity of the IR_{225}-signal the laboratory dose for the fine-grain test was increased (from 100 s for the IRSL tests) to 400 s. Such measure was not necessary for the coarse-grain samples, which for IR_{225} showed an increase in signal intensity as compared to IR_{60}. The $pIR_{1st}IR_{2nd}$-tests of the fine grains were performed still under the erroneous assumption that a pause-input of 10 s in the sequence editor adds a delay-time of 10 s in the measurement. This is why these measurements, too, show an excess of prompt readouts (zero-values on the x-axis). Only for the $pIR_{60}IR_{225}$-test on the coarse grains the shorter delay times were elongated. In addition, the maximum delay time was enlarged to ca. 80 h, as compared to ca. 10 h for the IRSL tests and ca. 20 h for the $pIR_{60}IR_{225}$-tests on the fine grains.

The differing times of laboratory irradiation result in differing values for tc and the differing maximum delay times further modulate the period („decades“) covered on the x-axis. Further, tc for IR_{225} is always larger than tc for IR_{60} of the same $pIR_{60}IR_{225}$-measurement, as the IR_{60}-readout (duration 240 s) precedes the IR_{225}-readout. This leads to a comparably shorter decade-coverage of IR_{225} as comapred to IR_{60}. Details of the SAR protocols are given in **Table ii** of the appendix. These explain the variations in decade-coverage. However, these variations are not crucial for the overall shape of the fading curves of the $pIR_{60}IR_{225}$-tests, which are shown in **Fig. 5 – 6** (fine-grain sample HDS-511) and **Fig. 7 – 8** (coarse-grain feldspar samples).

4.2 Results

A a result

- The IR_{60} readouts of the coarse grain tests show few outlier data points (marked with red circles in **Fig. 7**) which, however, are not crucial for the issues adressed in the following.
- Most fading curves exhibit an initial part with a lower gradient in data values followed by a section with a stronger gradient. The data values of the initial part may scatter around 1 or even exceed this threshold value of the first measured data point. Values above 1 do not conform to the model of anomalous signal fading. In other cases, the initial plateaus or ridges are less well defined, but may show up as flat-stepped stairs. In this respect, $IR_{1st}IR_{2nd}$ measurements resemble IRSL measurements.
- IR_{60}-(semi-)plateaus appear shorter and/or less pronounced than their IRSL counterparts. This may be explained by the comparably larger tc-values. Additionally, this may result from stronger optical and thermal washing by the IR_{225}-readout accomplishing each SAR cycle.

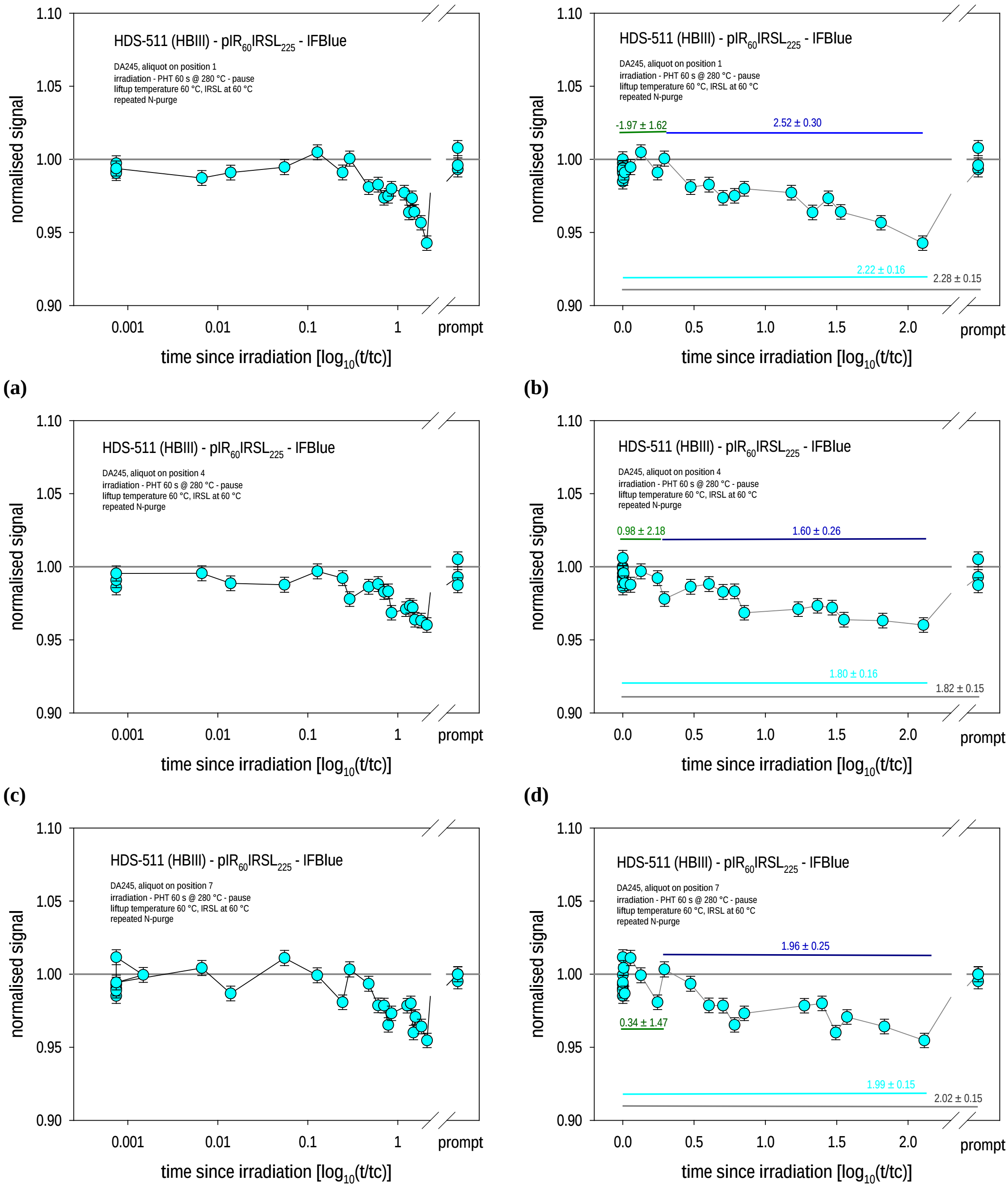

Fig. 5 $pIR_{60}IR_{225}$-fading measurement on polymineral fine-grain sample HDS-511 – here IRSL at 60 °C. SAR measurement with 400 s beta irradiation, 60 s preheating at 280 °C, pause, IRSL at 60 °C for 240 s and IRSL at 225 °C for 240 s. Repeated N-purge: 2 min N-purge at the end of each SAR cycle. Time since irradiation ($\log_{10}$[t/tc]) on a logarithmic scale with zero-values not presentable (**left**) and on a linear scale (**right**). tc is 584 s. All g-values normalised to 2 days. Longest delay time ca. 20 h.

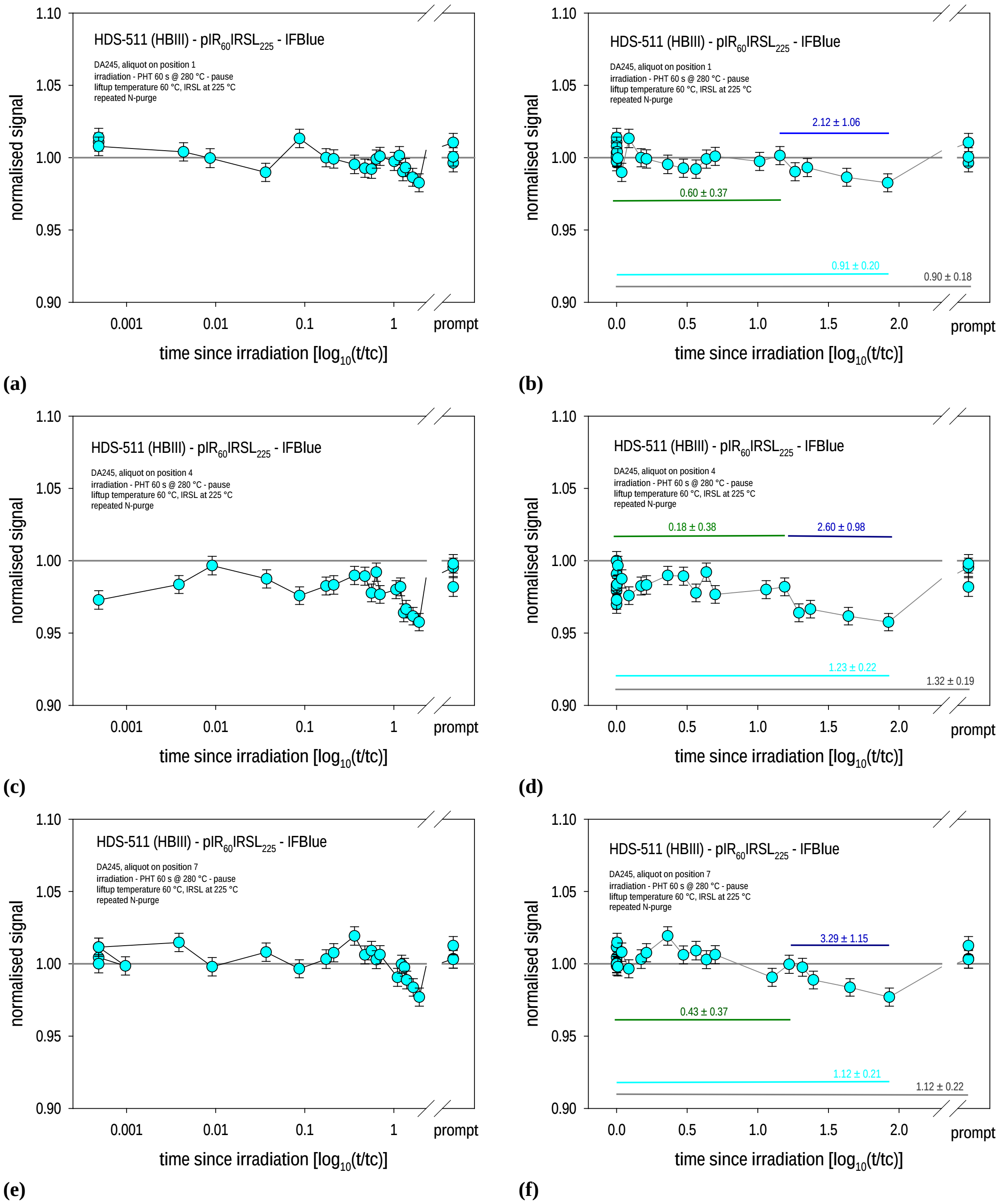

Fig. 6 pIR60IR225-fading measurement on polymineral fine-grain sample HDS-511 – here IRSL at 225 °C. SAR measurement with 400 s beta irradiation, 60 s preheating at 280 °C, pause, IRSL at 60 °C for 240 s and IRSL at 225 °C for 240 s. Repeated N-purge: 2 min N-purge at the end of each SAR cycle. Time since irradiation ($\log_{10}$[t/tc]) on a logarithmic scale with zero-values not presentable (**left**) and on a linear scale (**right**). tc is 893 s. All g-values normalised to 2 days. Longest delay time ca. 20 h.

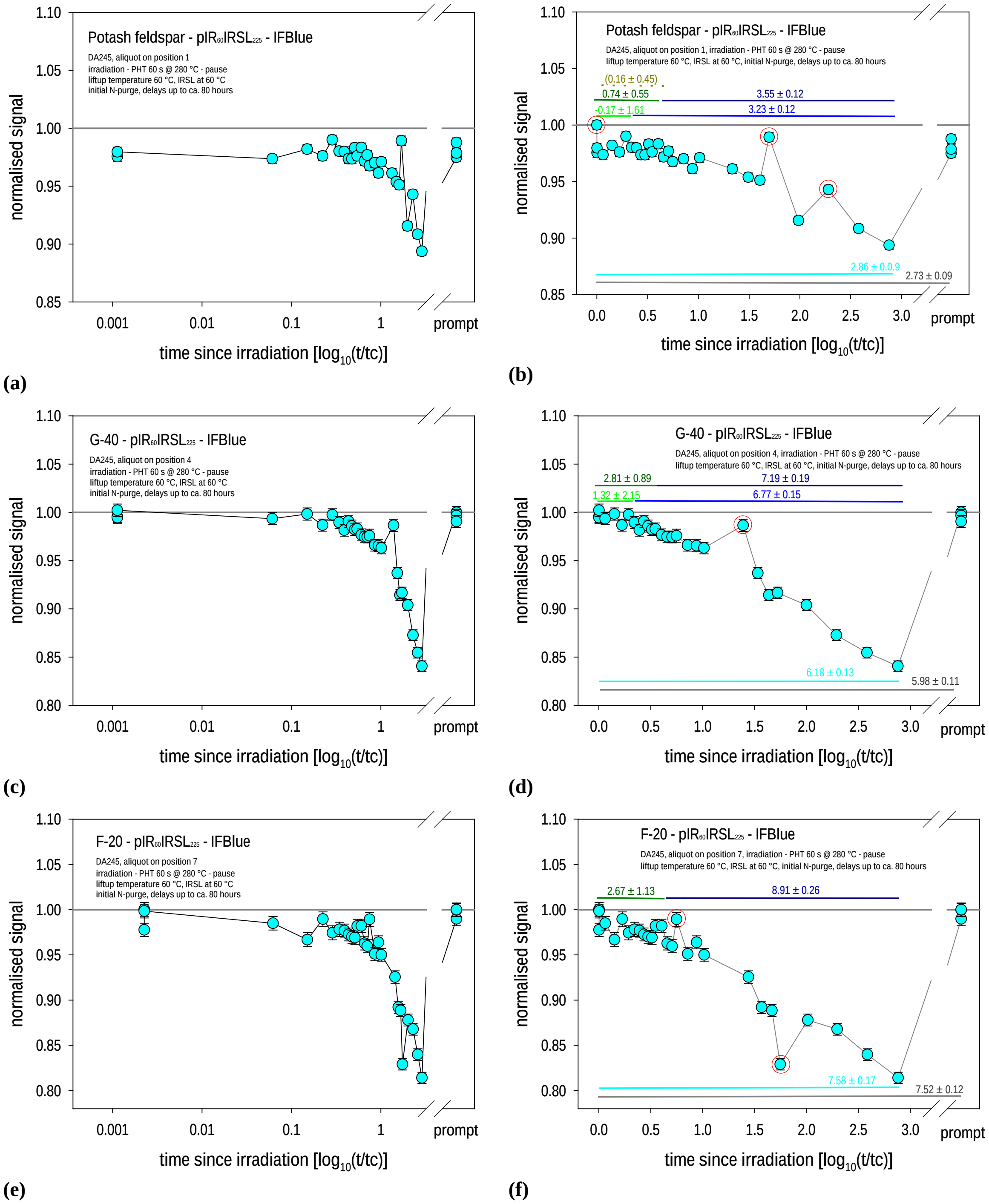

Fig. 7 $pIR_{60}IR_{225}$-fading measurement on coarse-grain (150 – 200 µm) feldspars – here IRSL at 60 °C. SAR measurement with 200 s beta irradiation, 60 s preheating at 280 °C, pause, IRSL at 60 °C for 240 s and IRSL at 225 °C for 240 s. 2 min N-purge at the start of the measurement. Time since irradiaton [$\log_{10}$(t/tc)] on a logarithmic scale with zero-values not presentable **(left)** and on a linear x-scale (**right**). Red circles denoting outliers. tc is 584 s. All g-values normalised to 2 days. Maximum delay time ca. 80 h. **(b)** Olive line signature and numbers in brackets g-value without very first outlier data point.

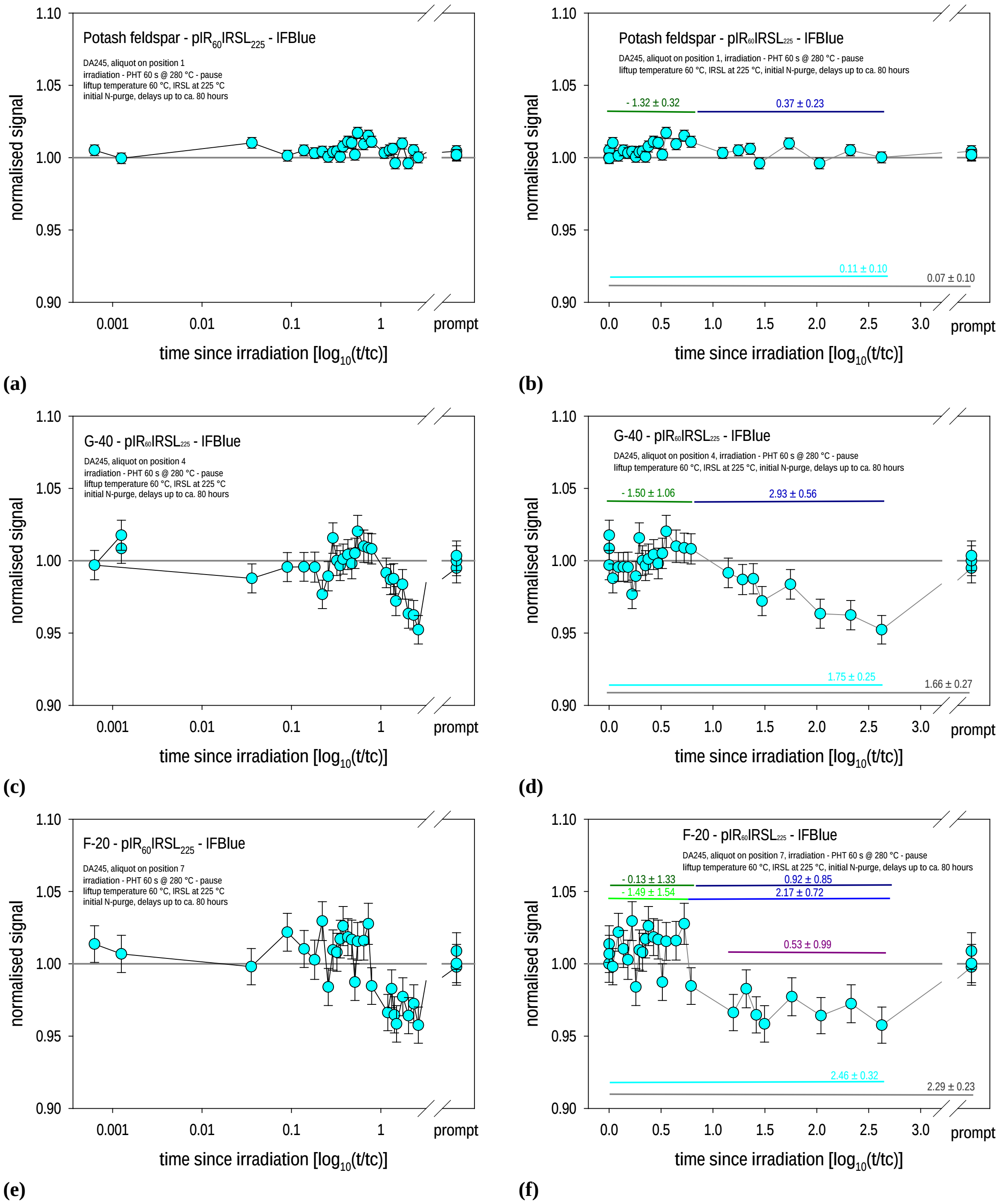

Fig. 8 pIR$_{60}$IR$_{225}$-fading measurement on coarse-grain (150 – 200 µm) feldspars – here IRSL at 225 °C. SAR measurement with 200 s beta irradiation, 60 s preheating at 280 °C, pause, IRSL at 60 °C for 240 s and IRSL at 225 °C for 240 s. 2 min N-purge at the start of the measurement. Time since irradiaton [log$_{10}$(t/tc)] on a logarithmic scale with zero-values not presentable **(left)** and on a linear x-scale (**right**). tc is 692 s. All g-values normalised to 2 days. Maximum delay time ca. 80 h.

- IR$_{225}$-(semi-)plateaus are longer than the IR$_{60}$-(semi-)plateaus, which may be caused by thermal and IR stimulation by the preceding IR$_{60}$-readout.
- Next to an initial plateau IR$_{225}$-readouts can show a rather flat gradient also for longer delay times (**Fig. 7b & 7f**). For the potash feldspar the g-value for the complete data set is still around zero, as the difference in level between the initial plateau and the later values is minimal. For the F-20 feldspar, however, for which the initial plateau ends quite abruptly

the difference is much larger. Taking into account data points representing both levels leads to an erroneously large g-value. Therefore, this example seems to illustrate how measurement artifacts for IR_{2nd}-g-values can be produced. Whether the gradient of the data values representing longer delay times of the G-40 feldspar (**Fig. 7d**) represents the fading rate, or whether (in part) it is overprinted by electron redistribution could perhaps be clarified with the measurement of longer delay times. It appears that the shape of a fading curve is dependent on the degree to which the electron redistribution plateau reaches above the later part of the fading curve (little for the potash feldspar, noticeable for the F-20 feldspar) and whether the initial plateau ends more abruptly (F-20 feldspar) or expires more gradually (perhaps G-40 feldspar?).

Conclusion

Our fading measurements with unusually short delay times often exhibit an initial part of the fading curve with a comparably small gradient, often with g-values around 0.

We observed initial (semi-)plateaus for IRSL at 60 °C as well as IR_{60} and IR_{225} in the frame of an $IR_{1st}IR_{2nd}$-SAR protocol. The length of the initial (semi-)plateau proofed comparably longer for IR_{2nd} than for IR_{1st}, likely promoted by electron excitation through the IR- and thermal stimulation of the preceeding IR_{1st}-readout.

Our earlier observations of an initial (semi-)plateau in the data curves of IRSL SAR fading tests on polymineral fine grains (as shown in the manuscript) apply also to $pIR_{1st}IR_{2nd}$ SAR fading tests both on (1) polymineral fine grains and (2) feldspar coarse grains (as shown in the final response). The latter allow an insight into how g-value artifacts may be generated for IR_{2nd}.

Several reasons are possible for an initial plateau in the fading curve: Tunneling afterglow or tunneling luminescence was observed after laboratory irradiation (Visosekas 1985, 1993; Molodkov et al. 2007). Huntley & Lamothe (2001) argue that the fading model based on tunneling of trapped electrons to nearby recombination centers does not apply for very short delay times after irradiation, due to the discrete nature of the crystal lattice and the low probability of very short distances between trap and center which would correspond to very quick recombination. These explanations are consistent with the occurance of an initial plateau. The plateau could also be a result of electron redistribution due to preheating (Auclair et al. 2003). As, however, both the fading test variants with preheating immediately after laboratory irradiation and preheating immediately before IR-readout produced a plateau, another charge-transfer process likely aids the plateau generation. Electron band-tail hopping (Guérin and Visocekas, 2015) might be a relevant mechanism. The longer IR_{225}-plateau could also be descriptively explained by the use-up of nearby recombination centers through the preceding IR_{60} stimulation. More distant electron-hole pairs then recombine only after prolonged delay times, in agreement with a longer initial plateau of the fading curve.

The occurance of an initial (semi-)plateau raises the question whether prompt readouts should be included in a g-value estimation and whether the first data point of a fading curve should be delayed sufficiently – after the end of a likely plateau. The inclusion of prompt readouts may be especially disadvantageous for IR_{2nd}-g-values in the frame of $pIR_{1st}IR_{2nd}$ SAR fading tests and explain to some extent why IR_{2nd}-g-values can be erroneously large.

References

Aitken, M.J.: An Introduction to Optical Dating, Oxford University Press, London, 267 pp, 1998.

Auclair, M., Lamothe, M., Huot, S.: Measurement of anomalous fading for feldspar IRSL using SAR. Radiation Measurements, 37, 487–492, https://doi.org/10.1016/S1350-4487(03)00018-0, 2003.

Huntley, D.J., Lamothe, M.: Ubiquity of anomalous fading in K-feldspars and the measurement and correction for it in optical dating, Canadian Journal of Earth Sciences 38, 1093-1106, https://doi.org/10.1139/e01-013, 2001.

Kadereit, A., Kühn, P., Wagner, G.A.: Holocene relief and soil changes in loess-covered areas of south-western Germany: The pedosedimentary archives of Bretten-Bauerbach (Kraichgau), Quaternary International 222 (1-2), 96 – 119, https://doi.org/10.1016/j.quaint.2009.06.025, 2010.

Kreutzer, S., Burow, C.: analyse_FadingMeasurement(): Analyse fading measurements and returns the fading rate per decade (g-value). Function version 0.1.14. In: Kreutzer, S., Burow, C., Dietze, M., Fuchs, M.C., Schmidt, C., Fischer, M., Friedrich, J., 2020. Luminescence: Comprehensive Luminescence Dating Data Analysis. R package version 0.9.8.9000-17. https://CRAN.R-project.org/package=Luminescence, 2020.

Molodkov, A., Jaek, I., Vasilchenko, V.: Anomalous fading of IR-stimulated luminescence from feldspar minerals: Some results of the study, Geochronometria, 26, 11–17, https://doi.org/10.2478/v10003-007-0007-0, 2007.

Murray, A.S., Wintle, A.G.: Luminescence dating of quartz using an improved single aliquot regenerative-dose protocol, Radiation Measurements, 32, 57–73, https://doi.org/10.1016/S1350-4487(99)00253-X, 2000.

Rhodius, C., Kadereit, A., Siegel, U., Schmidt, K., Eichmann, R., Khalil, L.A.: Constraining the time of construction of the irrigation system of Tell Hujayrat al-Ghuzlan near Aqaba, Jordan, using high-resolution optically stimulated luminescence (HR-OSL) dating, Archaeological and Anthropological Sciences, 9 (3), 345 –370, https://doi:10.1007/s12520-015-0284-x, 2015 (first online).

Thiel, C., Buylaert, J.-P., Murray, A., Terhorst, B., Hofer, I., Tsukamoto, S., Frechen, M.: Luminescence dating of the Stratzing loess profile (Austria) – Testing the potential of an elevated temperature post-IR IRSL protocol, Quaternary International, 234, 23 – 31, https://doi.org/10.1016/j.quaint.2010.05.018, 2011.

Thomsen, K.J., Murray, A.S., Jain, M., Bøtter-Jensen, L.: Laboratory fading rates of various luminescence signals from feldspar-rich sediment extracts, Radiation Measurements, 43, 1474–1486, https://doi.org/10.1016/j.radmeas.2008.06.002, 2008.

Visocekas, R.: Tunnelling radiative recombination in labradorite: its association with anomalous fading of thermoluminescence, Nuclear Tracks and Radiation Measurements, 10 (4–6), 521–529, https://doi.org/10.1016/0735-245X(85)90053-5, 1985.

Visocekas, R.: Tunneling radiative recombination in K-feldspar sanidine, Nuclear Tracks and Radiation Measurements, 21, 175–178, https://doi.org/10.1016/1359-0189(93)90073-I, 1993.

Table i Coarse-grain feldspar used for a $pIR_{60}IR_{225}$ SAR fading test and analytical data from the DigitalFire.com Reference Library.

Material	Grain-size fraction	Sieved again	K_2O [weight-%]	Na_2O [weight-%]	CaO [weight-%]
Norfloat Potash Feldspar 371214 (Cookson Matthey)	150 µm < x < 200 µm	Yes (CM)	12.0	2.9	0.4
G-40 Feldspar (Feldspar Corporation)	150 µm < x < 200 µm	Yes (CM)	10.4	3.0	0.8
F-20 Feldspar (Feldspar Corporation)	150 µm < x < 200 µm	Yes (JA)	4.1	6.82	1.4

- Source of information: DigitalFire.Com Reference Library:
- G-40 Feldspar: https://digitalfire.com/4sight/material/g-40_feldspar_801.html
- F-20: https://digitalfire.com/material/f-20+feldspar
- Norfloat Feldspar: https://digitalfire.com/material/norfloat+feldspar

Table ii Specifications of the IRSL- and $pR_{60}IR_{225}$-SAR protocols. Measurements on luminescence readers model Risø TL/OSL DA20: IRSL measurements on reader no. 240 („Athenaeum), $pR_{60}IR_{225}$ measurements on reader no. 245.

SAR protocol step				
	material	**polymineral fine grains**	**polymineral fine grains**	**feldspar coarse grains**
	protocol	**SAR IRSL**	**SAR pIR$_{60}$IR$_{225}$**	**SAR pIR$_{60}$IR$_{225}$**
	sample	**HDS-713**	**HDS-511**	**Potash feldspar, G-40, F-20**
[1]	**laboratory dose**	ß-IRR 100 s	ß-IRR 400 s	ß-IRR 200 s
[2]	**preheat procedure**	PHT 60 s at 250 °C (T_{fad}-13 to T_{fad}-16)	PHT 60 s at 280 °C	PHT 60 s at 280 °C
or		PHT 20 s at 280 °C (T_{fad}-17)		
or		PHT 60 s at 280 °C (T_{fad}-18)		
[3]	**prompt and delayed readouts**	3 x prompt, …, max. ca. 10 h, 3 x prompt	3 x prompt, …, max. ca. 20 h, 3 x prompt	3 x prompt, …, max. ca. 80 h, 3 x prompt
[4a]	**IRSL-readout**	IRSL 240 s at 50 °C (T_{fad}-13 to T_{fad}-16)	IRSL 240 s at 60 °C	IRSL 240 s at 60 °C
or		IRSL 240 s at 60 °C (T_{fad}-17 to T_{fad}-18)		
[4b]			IRSL 240 s at 225 °C	IRSL 240 s at 225 °C
[5]	**normalisation dose (test dose)**	ß-IRR 50 s	ß-IRR 200 s	ß-IRR 100 s
[6]	**preheat procedure**	PHT 60 s at 250 °C (T_{fad}-13 to T_{fad}-16)	PHT 60 s at 280 °C	PHT 60 s at 280 °C
or		PHT 20 s at 280 °C (T_{fad}-17)		
or		PHT 60 s at 280 °C (T_{fad}-18)		
[7a]	**IRSL-readout**	IRSL 240 s at 60 °C	IRSL 240 s at 60 °C	IRSL 240 s at 60 °C
[7b]			IRSL 240 s at 225 °C	IRSL 240 s at 225 °C
	tc	tc_{IRSL} 279 s (T_{fad}-13, -15), 263 (T_{fad}-14), 280 - 281 (T_{fad}-16), 223-224 (T_{fad}-17), 265 s (T_{fad}-18)	tc_{IR60} 583 - 584 s tc_{IR225} 892 - 893 s	tc_{IR60} 383-384 s tc_{IR225} 692 s